

# Design of a Highly Biomimetic Anthropomorphic Robotic Hand towards Artificial Limb Regeneration

Zhe Xu and Emanuel Todorov

**Abstract**—A wide range of research areas, from telemanipulation in robotics to limb regeneration in tissue engineering, could benefit from an anthropomorphic robotic hand that mimics the salient features of the human hand. The challenges of designing such a robotic hand are mainly resulted from our limited understanding of the human hand from engineering point of view and our ability to replicate the important biomechanical features with conventional mechanical design. We believe that the biomechanics of human hand is an essential component of the hand dexterity and can be replicated with highly biomimetic design. To this end, we reinterpret the important biomechanical advantages of the human hand from roboticist’s perspective and design a biomimetic robotic hand that closely mimics its human counterpart with artificial joint capsules, crocheted ligaments and tendons, laser-cut extensor hood, and elastic pulley mechanisms. We experimentally identify the workspaces of the fingertips and successfully demonstrate that our proof-of-concept design can be teleoperated to grasp and manipulate daily objects with a variety of natural hand postures based on hand taxonomy.

## I. INTRODUCTION

The significance of designing anthropomorphic robotic hands most likely originates from the expectation of using motorized prosthetic hand to restore lost hand dexterity. Although there is still no consensus about the definition of human hand dexterity, the biological variations found in length of bones, branching of tendons, and insertion of muscles [1] all suggest that dexterity is a highly personal property that is not only shaped by individual’s motor control ability, but also inherently bonded to the unique biomechanical characteristics of its very owner, and therefore can not be generalized without considering the biological difference.

The conventional approach to designing anthropomorphic robotic hands often involves mechanizing biological parts with hinges, linkages, and gimbals in order to simplify the seemingly complicated human counterparts. This approach is helpful for understanding and approximating the kinematics of the human hand in general, but inevitably introduces undesirable discrepancies between the human and robotic hands. The unique biomechanics of any abled human being, which includes complicated shapes of bones, varied rotational axes, and other biomechanical advantages, can be seen as a validated physical system as a whole. But most of these salient features are discarded in the mechanizing process. Although significant amount of efforts have been made by researchers to solve this mismatch from the control

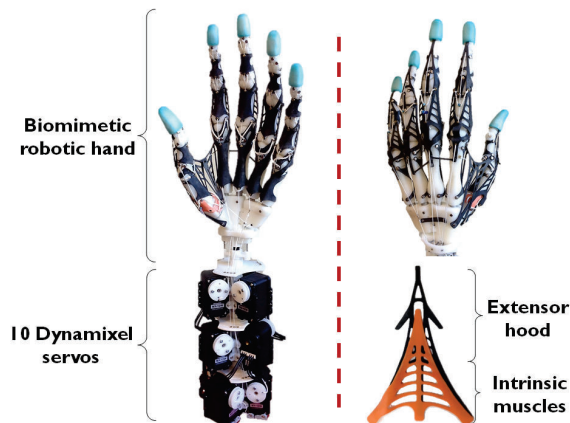


Fig. 1. The fully assembled biomimetic robotic hand. *Left*: The palmar aspect of the biomimetic robotic hand system. *Top right*: The dorsal view of the robotic hand. *Bottom right*: The laser-cut extensor hood integrated with intrinsic muscles. *Note*: The total weight of our biomimetic robotic hand is less than 1 kg (942 grams) including the actuation system.

and sensing aspects, very few work has been done to reduce the gap from the biomechanical point of view.

The general approach of our proposed method is first to identify the important biomechanical information of the human hand and then biomimetically replicate it. This allows a close replica that shares the same kinematic and even dynamic properties of its human counterpart. Our design benefits from several important rapid prototyping technologies: the shape of bones could be first captured with laser/MRI scanner and then 3D-printed with detailed surface features such as joint shapes and tendon insertion sites; soft tissues can be mimicked by using compliant silicone rubbers whose mechanical properties match that of the skin.

As shown in Fig.1, our approach resulted in a highly biomimetic anthropomorphic design, which will have potential impact on studies in both robotics and biology fields. Besides the obvious application in telemanipulation in which human operator can directly transfer his/her own dexterity to the robotic hand, it could also help medical and biology research in terms of physically preserving personal biomechanical data and serving as the 3D scaffolds for limb regeneration research.

In the following sections, we first review related work and introduce our design motivation. And then we reinterpret the important biomechanics of the human hand from engineering point of view. Meanwhile, we detail the biomimetic design and prototyping process of our anthropomorphic robotic hand. After this, we experimentally investigate the workspaces of each finger and the thumb. At the end, we

experimentally demonstrate the efficacy of our proof-of-concept design through grasping and manipulation experiments.

## II. RELATED WORK AND MOTIVATION

In order to properly position our proposed biomimetic robotic hand design, in this section we first briefly review the most relevant past work in robotics, and then explain the potential application of the highly biomimetic robotic hands in medical and biology research, to which end we formed our design concept.

### A. Anthropomorphic robotic/prosthetic hands

Many advanced anthropomorphic robotic hands have been developed during the past decade. As thoroughly summarized in a recent review [2], each of them possesses distinctive features in terms of actuation speed, magnified fingertip forces, or high degrees of freedom (DOFs), etc. However they all share the same design concept of mechanizing the biological counterparts. Their design ideas can be traced back to the technologies developed for industrial assembly robots. Equipped with joint and tactile sensors, the motion of such a human-like robotic hand can be seen as the coordination of five miniaturized high-precision industrial robots packed within a palm-sized space. The development of the anatomically corrected testbed (ACT) hand [3] was the first try towards replicating the human hand on anatomical level. However its internal mechanisms are still based on hinges and gimbals, we therefore categorize it as a special type of anthropomorphic robotic hand. The inherent mismatch between mechanisms of these robotic hands and biomechanics of human hands essentially prevents us from using natural hand motion to directly control them. Thus none of them can achieve the human-level dexterity yet.

The development of prosthetic hands heavily relies on the lessons we learned from building anthropomorphic robotic hands. State-of-the-art prosthetic hands can now be controlled with two different methods: Using non-intrusive methods such as electromyography (EMG) signals collected from the residual limb or targeted muscle reinnervation regions [4]; or using intrusive methods like directly implanting microelectrodes at the motor cortex of the brain [5] or cuffing peripheral nerves with miniaturized electrodes to collect control inputs [6]. The control of prosthetic hands essentially relies on human brain. Therefore the same neuroprosthetic technologies could be more effective if the design of the prosthesis could be more similar to its biological counterpart.

In contrast to these previous designs, we propose to use a highly biomimetic design to preserve the salient features of the human hand. Our design aims to minimize the design mismatch between robot and human hands for a more efficient control and a wider application.

### B. Design tools for medicine & biology research

We envision our biomimetic hand to become a useful tool in medicine and biology research. Transplanted hand is the only existing biological alternative for a lost human hand to

date. Yet the long-waiting list and the slim chance of finding the right donor keep preventing the method to be regularly practiced at hospitals. And there are still on-going debates about the lifelong rejection side-effects. In recent years, biologists start to investigate the possibility of regrowing tissues and organs through biofabrication: biocompatible materials can now be printed to form bone structures [7], biodegradable artificial ligaments have been used to replace the torn anterior cruciate ligaments [8], human muscles have been successfully cultivated inside petri dish [9], and peripheral nerves can also be regenerated given the right conditions [10]. All of these promising technologies require suitable scaffolds for the growth of grafted cells. When it comes to regrowing centimeter scale limbs, such as the rat forelimb, decellularised cadaver parts are required as scaffolds [11]. However even if the same techniques can be scaled up for human trails, the limitation of donors could eventually become a bottleneck. Besides, in medical research most of the in-vivo studies conducted on cadaver hands face constantly changing conditions since the decay process of the organic tissues is irreversible. The problem of biological variations caused by individual differences could also result in a long lasting debate. These limitations and drawbacks motivate us to seek for an alternative form of scaffold that can reliably preserve the biomechanical information of human hand in a physical working model.

An biomimetic anthropomorphic robotic hand that mimics the biomechanics of the human hand can be first validated in robotics lab and then mass-produced with biocompatible materials to meet the requirement of different medical/biological applications. While it is often regarded unnecessary to directly copy the bio-blueprint of the biological counterparts, it is possible to replicate critical biomechanical features of the human hand step by step. The key of success lies in a thorough understanding of the biomechanics of the human hand from the engineering point of view and the ability to materialize the findings.

## III. DEVELOPMENT OF THE HIGHLY BIOMIMETIC ROBOTIC HAND

In this section, we identify the important biomechanical features that shape the movement of human hand from the following aspects: the bones, joints, ligaments, tendons, extensor hood, and tendon sheaths. Instead of examining the human hand directly from a hand surgeon's perspective, in each of the following subsection we explain the essential hand biomechanics in engineering language and then discuss the ways to replicate these features with our biomimetic design.

### A. The bones and joints

As shown in Fig. 2, the human hand has four fingers and one thumb and is composed of 27 bones containing 8 tightly packed small wrist bones<sup>1</sup>. Each finger consists of

<sup>1</sup>We are interested in understanding the joint mechanism that enables finger movement, so the wrist bones (except for the trapezium bone) are not in scope of our investigation at this stage.

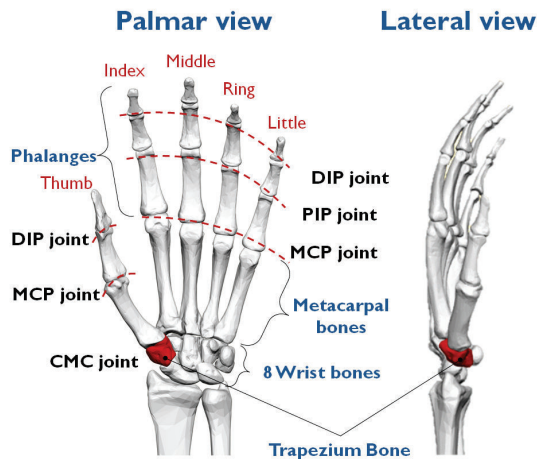


Fig. 2. The definition of the bones and joints of the human left hand (modified from [12]). Note: The trapezium bone is shown in red.

three phalanges and one metacarpal bones. The thumb is an exception, it only has two phalanges besides the metacarpal bone. But the opposable thumb accounts for a big portion of the entire hand function. The trapezium bone located at the base of the thumb has been found to be the critical component that enables the thumb opposition (labeled in red in Fig. 2). Together with the thumb's metacarpal bone, they form the carpometacarpal (CMC) joint of the thumb.

A joint is the connection between two adjacent bones whose shared contacting surfaces determine the possible motions of the joint. Different types of joints facilitate a different set of finger motions, known as the range of motion (ROM). The metacarpophalangeal (MCP) joints are formed by the connection of phalanges to the metacarpals. Depending on the distance to the MCP joint, there exist two more types of joints, namely, the proximal interphalangeal (PIP) joint and distal interphalangeal (DIP) joint. Based on this definition, the thumb only has one DIP joint between the two thumb phalanges. During the bending motion, the three finger joints work as mechanical hinges. However, the MCP joints have one extra set of active ROM that allows the finger to move from side to side, which are known as the abduction and adduction (ad/b) motions. In addition, the MCP joints also have one passive ROM that permits twisting motion around the axis of the finger phalanges. Thus, in the case of four fingers, we are only going to focus on describing the mechanism of the MCP joint, since the 1-DOF PIP and DIP joints can be seen as a simplified case. Different from the fingers, the complicated thumb movements are resulted from the contact between the trapezium and first metacarpal bones at the CMC joint. Due to the irregular shape of the trapezium bone (see Fig. 3), the exact locations of its joint axes are still under debate, but the CMC joint has been commonly explained as a saddle joint that allows the thumb to have a wide ROM - up (adduction) and down (abduction), bent (flexion) and straightened (extension), and the ability to move across the palm (opposition).

When designing robotic hands, robotics researchers often

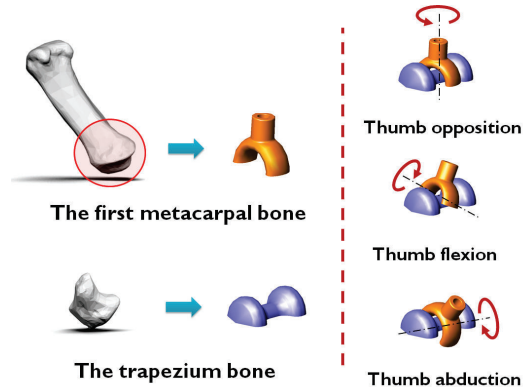


Fig. 3. Complicated bone shapes at the CMC joint of the thumb. Left: The common mechanical analogy of the first metacarpal and trapezium bones (shown in red, modified from [12]). Right: The fixed joint axes used for explaining different thumb movements.

choose 2-DOF universal joints for the MCP joints. The universal joint is good at transmitting rotary motion in shafts, but lacks the 1-DOF that allows the finger to passively twist with respect to the axial direction at the MCP joint. The same problem worsens when it comes to designing the CMC joint. Because the CMC joint requires not only saddle-shaped surfaces but also curved rotation axis that support rotation, sliding, translation, and pivoting motions [13]. Thus, none of the existing anthropomorphic robotic hands can restore the natural thumb motions with conventional mechanical joints that use fixed rotation axes. In addition, the irregular shapes of articular surfaces are also responsible for distributing stress. It is estimated that a tip pinch of 1 kg will generate 12 kg of joint compression at the CMC joint. For a power grip, the load could become as high as 120 kg [14].

In order to maximally preserve the important surface features of bones and joints, we 3D print artificial bones from the laser-scanned model of a cadaver skeleton hand [15]. As shown in Fig. 1, all finger segments of our robotic hand (excluding the actuator brackets) can be printed out on a  $20 \times 20$  cm tray (Dimension BST 768, Stratasys). Depending on the setting of the inner structure and resolution of the parts (0.025 mm), the total printing time could be less than 20 hours.

### B. The joint ligaments

The ROM at each finger joint is restricted by the length of ligaments. As shown in Fig. 4, ligaments are tough bands of fibrous tissues inserted on both sides of the two adjacent bones. Two important branches are called collateral ligaments. Similar structures can be found in all the finger joints with variations in length and thickness. Their function is to stabilize the joint, shape the ROM, and prevent abnormal sideways bending of each joint. For example, at the MCP joint, the collateral ligaments originate from the dorsal side of the metacarpal bone and end near the palmar side of the adjacent finger phalanx. In this way, the collateral ligaments get taut when the finger bends, and become relaxed once the finger straightens. This is why our index finger can easily move from side to side when it extends, but has very limited side motions once it fully bends. The thick ligament formed

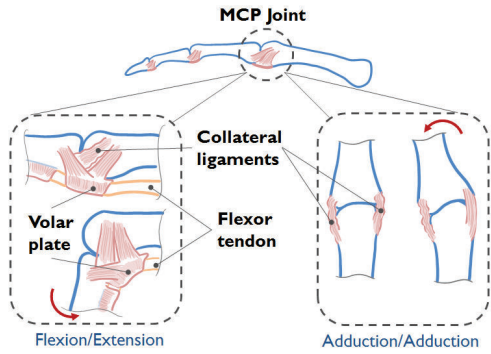


Fig. 4. Schematic showing the function of collateral ligaments and volar plate at the MCP joint.

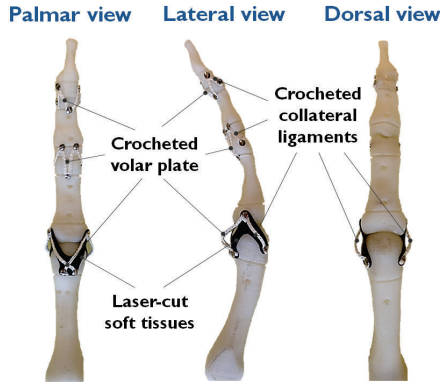


Fig. 5. The skeleton of the 3D-printed finger connected by crocheted ligaments and laser-cut joint soft tissues. *Note:* All the crocheted ligaments are anchored by 1 mm screws at their biological insertion sites.

on the palmar side of the finger is called volar plate. Like the collateral ligaments, the volar plate also has insertions on both sides of the bones. Its function is to prevent the occurrence of the finger deformity from hyper-extension. Together with other accessory ligaments and soft tissues, collateral ligaments and volar plate form important structure known as the joint capsule.

Our artificial joint capsule design allows each robotic finger to be quickly assembled as shown in Fig. 5. One pair of the crocheted ligaments is used to mimic the two collateral ligaments located on the sides of each finger joint. Similarly, the function of the volar plate is replaced by two crocheted ligaments anchored across each joint. Laser-cut rubber sheet is used to mimic the soft tissues providing the human-like compliance. Based on the ROM of each joint, the dimension of these components varies in size and length. Compared to our previously proposed joint design [16], our current design greatly reduced the fabrication time.

### C. Tendons and muscles

Between the bones and muscles, there are two groups of tendons in the human hand. The ones straightening the fingers are called extensor tendons, the ones bending the fingers are called flexor tendons. The excursion motions of the tendons originate from the corresponding muscle groups located in the forearm. If we treat the muscles as the actuators

that output contraction forces, the tendons of the hand serve as the transmission system that smartly partition the forces and smoothly deliver torques to each finger joint. As shown in Fig. 6(a), starting from the wrist, the extensor tendons branch out and have multiple insertion sites on the dorsal side of the finger bones. On the palmar side, after passing through the carpal tunnel, the flexor tendons (see Fig. 6(d)) travel through a series of pulley-like tendon sheaths grown onto the palmar side of the bones and eventually insert at the base of the DIP and PIP joints. The collaborative motions of the two tendon groups make fluent hand movement possible.

The large muscle groups that directly connect to the central branch of the flexor and extensor tendons are called extrinsic muscles. Most of them originate from the elbow and have muscle bellies located in the forearm. However there also exist several small muscle groups called intrinsic muscles that are often slim enough to reside in the gap between the two adjacent metacarpal bones. The majority of these small muscles start from the wrist of hand and connect to the thin branches (the extensor hood) of the extensor tendons of each finger near the MCP joint. One important function of these intrinsic muscles is to provide passive reflex-mediated stiffness at finger joints during various hand activities. We use resilient, laser-cut rubber sheet to mimic these small muscles as a joint stabilization mechanism (see Fig. 1).

In total, ten Dynamixel servos (nine MX-12W and one AX-12A) are used to mimic the important large muscles and actuate our proposed robotic hand (as shown in Fig. 1). Two servos are used to control the flexion and extension of the ring and little fingers through a differential pulley transmission (see Fig. 8). The index and middle fingers are separately controlled by two pairs of servos so that each of them can bend and straighten independently. In addition, they also share an extra servo for a coupled control at their MCP joints<sup>2</sup>. We use three actuators to control the thumb. One of them is an AX-12A Dynamixel servo that has a larger gear ratio (254/1) than others (32/1) and is used for the extension and abduction of the thumb. The other two servos of thumb are assigned to control the flexion and adduction motions, respectively. The palm has one underactuated DOF that relies on the flexion motion of the ring and little fingers. Although the wrist of the current version only serves as a static base for testing the fingers, its cable routing structure closely mimics the capral tunnel of the human hand.

### D. Extensor hood

Most of our daily tasks involving hand motions require the contraction of strong muscles connecting to the flexor tendons. Therefore during grasping, the extensor tendons mainly work as a breaking system that constantly regulates the torques at finger joints. The functionality of the breaking system relies on a fibrous structure known as the extensor hood. The extensor hood is a thin, complex, and collagen-based web structure that directly wraps around the finger

<sup>2</sup>In our current design, the abduction/adduction motion is passively regulated by the laser-cut intrinsic muscles integrated at the MCP joints for all the fingers

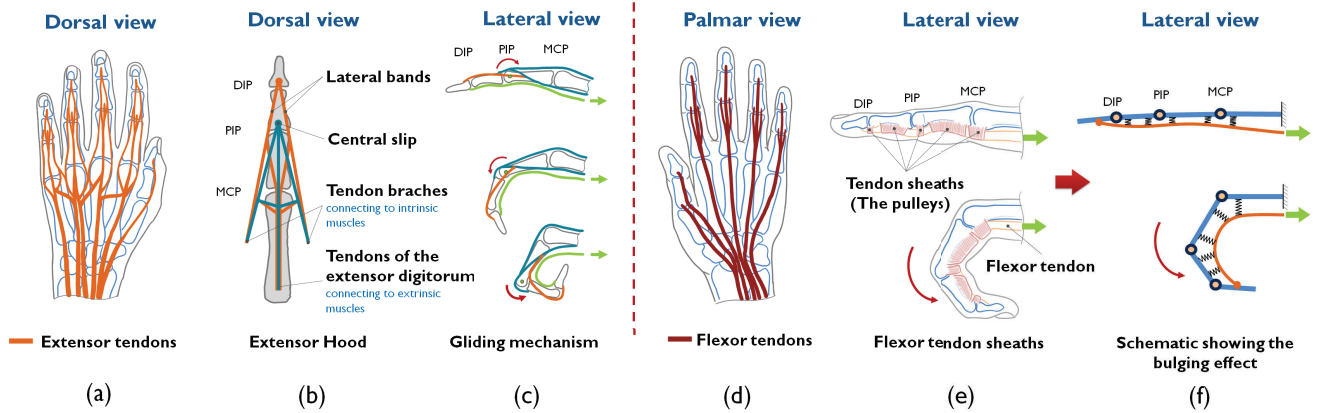


Fig. 6. The important biomechanical advantages of the extensor and flexor tendons of a human left hand. (a) Schematic drawing of the extensor tendons. (b) A simplified geometric representation of the extensor hood. (c) The regulation of torques at the PIP joint during finger flexion. (d) Schematic drawing of the flexor tendons. (e) The bulging process of the tendon sheaths (the pulleys) during finger flexion. (f) Mechanical analogy of the bending finger showing the increase in moment arms under the effects of elastic pulleys.

phalanges from the dorsal side. Its structure can be geometrically represented by a two-layer web as shown in Fig. 6(b).

The first layer of the extensor hood is called lateral bands. It has an insertion site at the base of the DIP joint, and split into two small ligaments across the PIP joint. This splitting mechanism smartly regulates the breaking torques at the PIP joint based on different postures of the finger during its bending process (see Fig. 6(c)). As shown in the lateral view, when the finger straightens, the two small ligaments are above the rotation axis at the PIP joint serving as branches of the extensor tendons. When the flexor tendons keep pulling and extensor tendons getting stretched, the finger starts its bending process during which the two small ligaments continue to glide off from the PIP joint and eventually pass downwards the rotation axis. Hereinafter, although the extensor tendons are still transmitting forces into the two small branches via the web structure, the two small branches are no longer behaving like extensor tendons at the PIP joint, but instead they begin to help flex the finger by providing increasing flexion torques at the PIP joint. When the finger straightens, the above process repeats in the reverse order.

The second layer of the extensor hood is known as the central slip with a insertion point at the base of the PIP joint. Its function is to help extend/flex the PIP joint. One of its tendon branches is often connected to a small intrinsic muscle, namely, the lumbrical muscle. It has been reported that the lumbricals work as flexor tendons at the MCP joints, but can help extend the PIP and DIP joints via the extensor hood mechanism. Due to its variations in size and inserting locations, the function of the lumbricals are not unanimously agreed yet. So we treat them as a part of the intrinsic muscles without emphasizing its uniqueness in Fig. Fig. 6(c). In sum, the complex, web structure of the extensor hood smartly transmits muscle forces to finger joints through the gliding mechanism.

As shown in Fig. 1, highly resilient rubber sheets are first laser cut into the shape of extensor hood (with intrinsic muscles integrated) and then attached to the skeleton of the

fingers (see Fig. 7) at biological insertion sites to mimic the passive behavior of the extensor hood, leaving servos to achieve the active extension of the finger through the gliding mechanisms. This is an important biomechanical advantage that we incorporated into our robotic hand design.

#### E. Tendon sheaths

As shown in Fig. 6(e), the tendon sheaths are fibrous tissues that wrap around the flexor tendons and have multiple insertions on the dorsal side of finger bones. Due to their important functions, each section of the tendon sheaths has been named after a numbered annular pulley in nomenclatures of hand anatomy based on their distances to the MCP joint. Mechanical engineers design different pulley systems to apply forces and transmit power through cables. The tendon sheaths in the human hand work as a series of elastic pulleys to help efficiently transmit flexion forces from the muscles to the joints. Since the tendon sheaths can flatten down when the finger straightens and bulge out when the finger bends [17].

As illustrated in Fig. 6(e) and (f), if the flexor tendon starts pulling a straightened finger with constant force and speed, the initial moment arms at joints are small and therefore can cause a fast bending motion of the finger but result in small flexion torques at the joints. However when the finger starts bending, the bulging effect of tendon sheaths greatly increases the moment arms at joints leading to a slowed finger motion with rapidly magnified flexion torques. With the elastic pulley system, the human hand can keep the torques at the finger joints small when approaching the object, but quickly deliver large torques to the finger joints when forming a grip. Combined with the gliding mechanisms, this is another biomechanical advantage that helps the flexor tendons to dominate the finger dynamics during flexion motions.

As shown in Fig. 7, three patches of laser-cut rubber sheets are used to mimic the elastic pulley mechanism. The flexor tendon made of high strength Spectra® strings

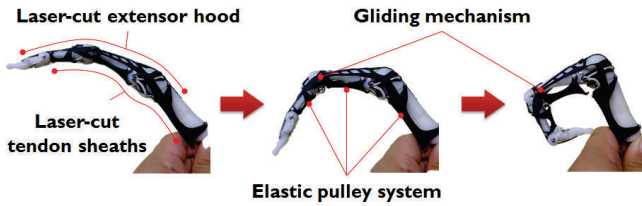


Fig. 7. Snapshots of an assembled finger showing both the gliding mechanism of the extensor hood and the bulging effect of the tendon sheaths during finger flexion.

(200 N yield strength) is routed through the rubber tendon sheaths via several rivet reinforced ports. The flexor tendons of our robotic hand mimic the flexor digitorum profundus (FDP) tendon of human hand. Although the human finger has another flexor tendon - the flexor digitorum superficialis (FDS) tendon - inserted to the base of the PIP joint, we choose not to incorporate the FDS in this version of the robotic hand, because it is reported that the FDP tendon generates greater fingertip forces than the FDS tendon during isometric tasks [18].

#### IV. PERFORMANCE OF THE BIOMIMETIC ROBOTIC HAND

In order to evaluate the efficacy of our proof-of-concept design, in this section, we first quantitatively investigate the fingertip trajectories, and then qualitatively conduct the telemanipulation experiments. The experimental setup, procedures, and results are reported in following subsections.

##### A. Fingertip trajectories

As we briefly mentioned, the ring and little fingers are coupled considering their collaborative relationship as the grasping fingers. Their flexion and extension motions are controlled by a pair of Dynamixel servos through a differential pulley transmission as shown in Fig. 8. The benefit of using such a pulley structure is to provide an extra source of hand compliance in addition to the build-in compliance at each finger joint, since it allows the two grasping fingers to conform to the contour of an object by automatically adjusting the shared string length between the two insertion sites. But the drawback is that the underactuated mechanism could also become a source of uncertainty bringing the two fingers into certain unknown postures when they bend and straighten between the two extreme postures. Thus it is important to first investigate the repeatability of our proposed mechanism, especially when the finger's ROM is controlled in between full flexion and extension postures.

Compared to the ring and little fingers, the index, middle, and thumb are each actuated by more than two servos, therefore they can be better controlled in this case. In the fingertip tracking experiment, we chose two extreme positions for the coupled ring and little fingers, and then controlled the two servos to bend and straighten the coupled fingers approximately once every two seconds. The coordinates of the reflective markers attached to the fingertip are recorded by a motion capture system (Vicon Bonita)

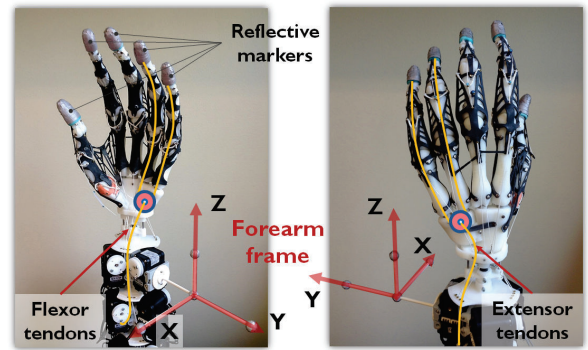


Fig. 8. Labeled pictures showing the differential pulley transmission for ring and little fingers and the locations of the reflective markers. *Note:* All the marker coordinates were recorded with respect to the forearm frame.

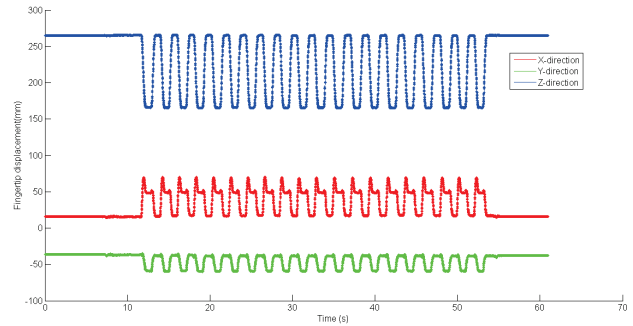


Fig. 9. The displacement of the ring's fingertip during 20 repetition of flexion and extension motions. *Note:* Similar tracking data were recorded and observed for the little finger.

composed of 7 infrared cameras at 240 Hz VGA resolution. The Vicon system was calibrated, and is able to detect 0.5 mm displacement in all directions.

In order to avoid the marker occlusion and confusion issues, we attached a forearm frame (see Fig. 8) near the wrist of our robotic hand, so that we could record the marker trajectories for one fingertip at a time, and then transform their coordinates from the default world frame to this forearm frame when processing the data. The use of this forearm frame also allows us to constantly change the orientation of our robotic hand during hand motions in order to achieve good visibility for the reflective markers.

The Cartesian coordinates of the fingertips from the ring and little fingers are very similar, and therefore only the ones from the ring finger are plotted in Fig. 9. The data of 20 repetitions of the full flexion and extension motions show a highly repeatable pattern suggesting that our biomimetic finger design and the differential pulley system can be successfully combined to build reliable robotic hand.

After being projected onto the X-Z plane, the flexion and extension trajectories of the ring finger's tip can be clearly observed in Fig. 10(b). Our experiments show that the flexion and extension motions of our biomimetic robotic finger were not following the same trajectory. The area bounded by the two trajectories covers a big portion of the reachable workspace of the ring finger [19]. The flexion trajectory closely resembles that of the logarithmic spiral curve observed from human finger's flexion motion [20]. The

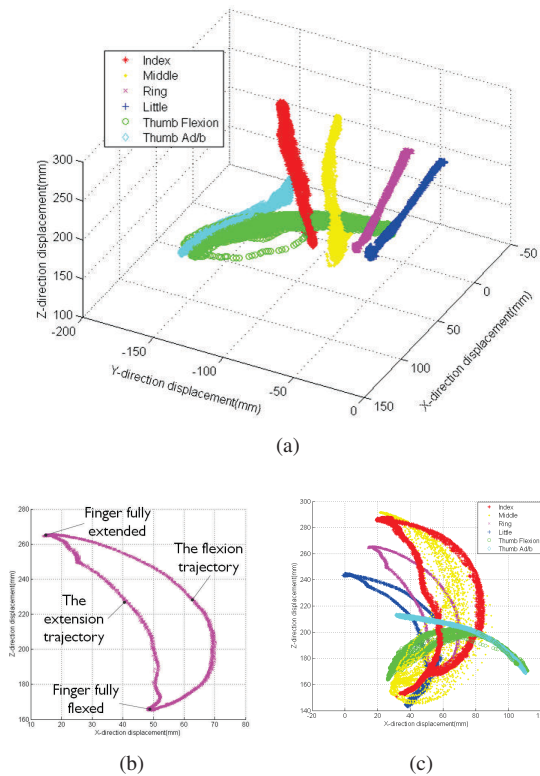


Fig. 10. The trajectories of the fingertips of our biomimetic robotic hand. (a) 3D scatter plot of fingertip trajectories. (b) The ring fingertip’s trajectories projected onto the X-Z plane. (Note: The scatter plot is from the 20 repetitions of the full flexion and extension motions.) (c) The trajectories of the fingertips projected onto the X-Z plane.

difference between the flexion and extension fingertip trajectories results from the sequential joint movements shaped by joint stiffness. As shown in Fig. 7, the variable joint stiffness is regulated by the gliding mechanism of the extensor hood and the elastic pulleys of the tendon sheaths.

The fingertip trajectories of other digits were also recorded. Unlike the pre-determined inputs for the ring and little fingers, the repetitive movements of the index, middle, and thumb were teleoperated by the human operator through our custom-made data glove<sup>3</sup>. As shown in Fig. 10, the two principal components of the thumb motions, namely the flexion/extension and the abduction/adduction were tested separately. The teleoperation results in more scattered data points compared to the ones collected from the preprogrammed motions of ring and little fingers (see Fig. 9).

### B. Object grasping and manipulation

In order to further evaluate the overall performance of our robotic hand, we conducted grasping and manipulation experiments using 31 objects from the prioritized list [21]. During the test a human operator hands different objects to the robotic hand with his right hand, meanwhile, used his left hand to teleoperate the digits of the robotic hand to grasp/manipulate the object via the data glove (see Fig. 11). This process is known as the tele-manipulation during which

<sup>3</sup>Details about the data glove can be found in [15], but is out of the scope of this paper.

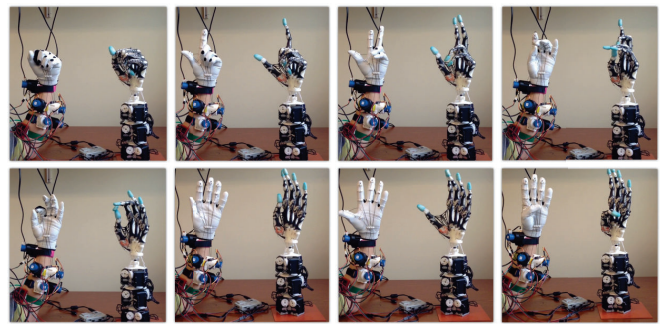


Fig. 11. Snapshots showing the teleoperation process of our biomimetic robotic hand.

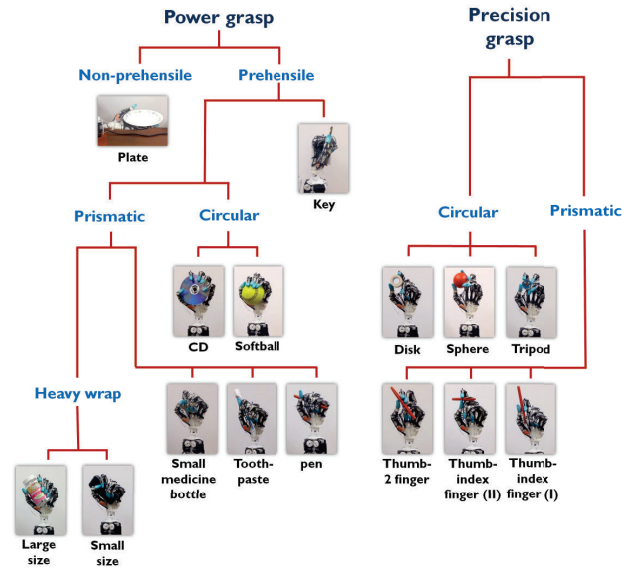


Fig. 12. The hand taxonomy realized by our biomimetic robotic hand (Note: see the taxonomy figure in [22] for comparison).

the movement of the robotic hand is both controlled and guided by the same human operator’s hand motion and visual feedback. This experiment can be seen as a series of cooperative grasping tasks between the human operator and the robotic hand in which the former could clearly monitor the status of the grasped object without the occlusion issue at the grasping site (see our video submission for details).

During the object grasping task, we observed that different grasping postures can be naturally transferred from the human operator to our biomimetic robotic hand, particularly from the motion of the thumb. This is because our biomimetic robotic hand successfully preserves the important biomechanics of the human hand that essentially determines the hand kinematics. The resulting grasps cover most of the grasping types defined by human hand taxonomy [22], except for the ones that require independent control of the ring and little fingers (see Fig. 12).

Last but not least, we tested the in-hand manipulation ability of our biomimetic robotic hand. As shown in Fig. 13, the whiteboard eraser was successfully regripped from horizontal to vertical position through a series of continuous hand motions involving the use of all the digits. It is interesting

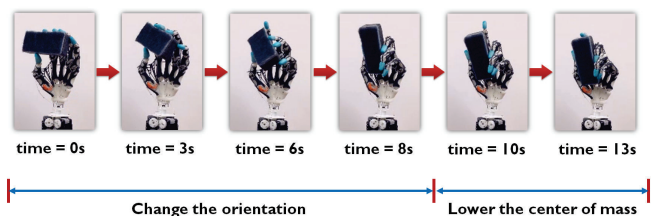


Fig. 13. Snapshots of our biomimetic robotic hand performing in-hand manipulation of a whiteboard eraser.

to observe that complicated in-hand manipulation tasks can be accomplished without any force feedback. This again suggests that matching the kinematics of the robotic hand to its human counterpart is important for the success of teleoperation tasks.

## V. CONCLUSION AND FUTURE WORK

We have designed and prototyped a highly biomimetic anthropomorphic robotic hand that closely mimics the important biomechanics of the human hand with artificial joints and ligaments. During this process, we first identified two crucial constraints that have been limiting the development of anthropomorphic robotic hands: the lack of properly translated engineering knowledge of the human hand and the restrictions caused by conventional mechanical joints. And then we reinterpreted and detailed the ways to replicate important biomechanical advantages of the human hand with the language and methods that roboticists can easily understand. We experimentally demonstrated that our proposed robotic hand design has good repeatability in finger motions and can be teleoperated to grasp and manipulate a wide selection of daily objects within the fingertip workspaces under current design.

In future work, we are planning to incorporate biomimetic wrist design and already-developed fingertip sensors [23] into our robotic hand so that we can further improve its telemanipulation performance. In addition, due to the inherent similarity between our robotic hand and its human counterpart, we are going to collaborate with researchers from biology and tissue engineering to further explore its potential to serve as a bio-fabricated device/scaffold in the emerging fields of neuroprosthetics and limb regeneration.

## VI. ACKNOWLEDGMENTS

This work was supported by the US National Science Foundation. The authors would like to thank Dr. Christopher Allan at the HarborView Medical Center for his help on guiding the cadaver hand dissection, and thank Svetoslav Kolev for his help on setting up Vicon experiments.

## REFERENCES

- [1] H.-M. Schmidt and U. Lanz, *Surgical anatomy of the hand*. Thieme, Stuttgart, 2004.
- [2] R. Balasubramanian and V. J. Santos, *The human hand as an inspiration for robot hand development*. Springer, 2014.
- [3] A. D. Deshpande, Z. Xu, M. J. V. Weghe, B. H. Brown, J. Ko, L. Y. Chang, D. D. Wilkinson, S. M. Bidic, and Y. Matsuoka, "Mechanisms of the anatomically correct testbed hand," *Mechatronics, IEEE/ASME Transactions on*, vol. 18, no. 1, pp. 238–250, 2013.

- [4] T. A. Kuiken, G. Li, B. A. Lock, R. D. Lipschutz, L. A. Miller, K. A. Stubblefield, and K. B. Englehart, "Targeted muscle reinnervation for real-time myoelectric control of multifunction artificial arms," *Jama*, vol. 301, no. 6, pp. 619–628, 2009.
- [5] J. L. Collinger, B. Wodlinger, J. E. Downey, W. Wang, E. C. Tyler-Kabara, D. J. Weber, A. J. McMorland, M. Velliste, M. L. Boninger, and A. B. Schwartz, "High-performance neuroprosthetic control by an individual with tetraplegia," *The Lancet*, vol. 381, no. 9866, pp. 557–564, 2013.
- [6] M. Ortiz-Catalan, B. Håkansson, and R. Brånemark, "An osseointegrated human-machine gateway for long-term sensory feedback and motor control of artificial limbs," *Science translational medicine*, vol. 6, no. 257, pp. 257re6–257re6, 2014.
- [7] M. J. Sawkins, P. Mistry, B. N. Brown, K. M. Shakesheff, L. J. Bonassar, and J. Yang, "Cell and protein compatible 3d bioprinting of mechanically strong constructs for bone repair," *Biofabrication*, vol. 7, no. 3, p. 035004, 2015.
- [8] Y.-K. Seo, H.-H. Yoon, K.-Y. Song, S.-Y. Kwon, H.-S. Lee, Y.-S. Park, and J.-K. Park, "Increase in cell migration and angiogenesis in a composite silk scaffold for tissue-engineered ligaments," *Journal of Orthopaedic Research*, vol. 27, no. 4, pp. 495–503, 2009.
- [9] L. Madden, M. Juhas, W. E. Kraus, G. A. Truskey, and N. Bursac, "Bioengineered human myobundles mimic clinical responses of skeletal muscle to drugs," *Elife*, vol. 4, p. e04885, 2015.
- [10] X. Gu, F. Ding, and D. F. Williams, "Neural tissue engineering options for peripheral nerve regeneration," *Biomaterials*, vol. 35, no. 24, pp. 6143–6156, 2014.
- [11] B. J. Jank, L. Xiong, P. T. Moser, J. P. Guyette, X. Ren, C. L. Cetrulo, D. A. Leonard, L. Fernandez, S. P. Fagan, and H. C. Ott, "Engineered composite tissue as a bioartificial limb graft," *Biomaterials*, vol. 61, pp. 246–256, 2015.
- [12] Wikipedia, "Trapezium (bone) — wikipedia, the free encyclopedia," 2014, [Online; accessed 12-May-2015]. [Online]. Available: [http://en.wikipedia.org/w/index.php?title=Trapezium\\_\(bone\)&oldid=634623814](http://en.wikipedia.org/w/index.php?title=Trapezium_(bone)&oldid=634623814)
- [13] J. J. Crisco, E. Halilaj, D. C. Moore, T. Patel, A.-P. C. Weiss, and A. L. Ladd, "In vivo kinematics of the trapeziometacarpal joint during thumb extension-flexion and abduction-adduction," *The Journal of hand surgery*, vol. 40, no. 2, pp. 289–296, 2015.
- [14] W. P. Cooney and E. Chao, "Biomechanical analysis of static forces in the thumb during hand function," *The Journal of Bone & Joint Surgery*, vol. 59, no. 1, pp. 27–36, 1977.
- [15] Z. Xu, "Design and control of an anthropomorphic robotic hand: Learning advantages from the human body & brain," Ph.D. dissertation, University of Washington, 2015.
- [16] Z. Xu, E. Todorov, B. Dellon, and Y. Matsuoka, "Design and analysis of an artificial finger joint for anthropomorphic robotic hands," in *2011 IEEE International Conference on Robotics and Automation (ICRA)*, 2011.
- [17] A. Amis and M. Jones, "The interior of the flexor tendon sheath of the finger: the functional significance of its structure," *Journal of Bone & Joint Surgery, British Volume*, vol. 70, no. 4, pp. 583–587, 1988.
- [18] K. Kursa, E. Diao, L. Lattanza, and D. Rempel, "In vivo forces generated by finger flexor muscles do not depend on the rate of fingertip loading during an isometric task," *Journal of biomechanics*, vol. 38, no. 11, pp. 2288–2293, 2005.
- [19] S. Venema and B. Hannaford, "A probabilistic representation of human workspace for use in the design of human interface mechanisms," *Mechatronics, IEEE/ASME Transactions on*, vol. 6, no. 3, pp. 286–294, Sep 2001.
- [20] D. G. Kamper, E. G. Cruz, and M. P. Siegel, "Stereotypical fingertip trajectories during grasp," *Journal of neurophysiology*, vol. 90, no. 6, pp. 3702–3710, 2003.
- [21] Y. S. Choi, T. Deyle, T. Chen, J. Glass, and C. Kemp, "A list of household objects for robotic retrieval prioritized by people with als," in *Rehabilitation Robotics, 2009. ICORR 2009. IEEE International Conference on*, June 2009, pp. 510–517.
- [22] M. R. Cutkosky, "On grasp choice, grasp models, and the design of hands for manufacturing tasks," *Robotics and Automation, IEEE Transactions on*, vol. 5, no. 3, pp. 269–279, 1989.
- [23] Z. Xu, S. Kolev, and E. Todorov, "Design, optimization, calibration, and a case study of a 3d-printed, low-cost fingertip sensor for robotic manipulation," in *Robotics and Automation (ICRA), 2014 IEEE International Conference on*. IEEE, 2014, pp. 2749–2756.